

# A complete method for efficient fuzzy modal analysis

F. Massa\*, K. Ruffin, T. Tison, B. Lallemand

*Laboratoire d'Automatique de Mécanique et d'Informatique industrielles et Humaines, Université de Valenciennes,  
Le Mont Houy B.P. 311, 59313 Valenciennes, France*

Received 20 December 2005; received in revised form 3 April 2007; accepted 17 April 2007  
Available online 27 September 2007

---

## Abstract

The objective of this paper is to determine both the fuzzy eigenvalues and eigenvectors of a finite element model defined with fuzzy parameters. The proposed method introduces the concepts of mode shape pairing and the functional dependence of eigensolutions with respect to design parameters. High-order approximations are then introduced to limit the computational cost associated with variability management. Numerical test cases are used to highlight the abilities of this method to predict behaviour modifications due to variations in the physical parameters.

© 2007 Published by Elsevier Ltd.

---

## 1. Introduction

In recent times, the development of computing resources has radically modified the type of problems accessible to simulations tools. Today, numerical simulations (e.g., the finite element method) are well established in industry and are essential in the design phase of mechanical structures. Although numerical models have become more and more complex and realistic, the results are still quite different from observed reality. Indeed, when realizing and using mechanical structures, the sources of variability and uncertainty [1] can be numerous. In this context, variability refers to the variation inherent to a given physical system or environment, and uncertainty refers to a potential deficiency in any modelling phase or activity that is due to lack of knowledge. Variability typically exists in terms of physical properties and manufacturing tolerances, while uncertainty is more a question of model inaccuracies. Variability and uncertainty inevitably affect the response of the structure and, therefore, its reliability.

Different approaches have been developed to take this variability and/or uncertainty into account. The probabilistic [2–4], interval [5,6], convex [7] and fuzzy approaches currently provide the principal tools for dealing with the variability and uncertainty commonly found in engineering problems. In this paper, fuzzy sets theory [8–12] is used. This formalism is based on the idea that the subset bounds are difficult to define precisely. Dubois and Prade [13] add that the values defining fuzzy sets do not produce a precise description, but rather reflect a tendency. Thus, this fuzzy formalism can be used to introduce the notion of variability in design parameters. In the literature, the first solution described for solving fuzzy modal analysis applied

---

\*Corresponding author. Tel.: +33 3275 11459; fax: +33 3275 11317.  
E-mail address: [franck.massa@univ-valenciennes.fr](mailto:franck.massa@univ-valenciennes.fr) (F. Massa).

Nomenclature	
$\mathbf{K}(\tilde{p}_1, \dots, \tilde{p}_n)$	stiffness matrix depending on fuzzy parameters $\tilde{p}_1, \dots, \tilde{p}_n$ (size $[N_{\text{dof}} \times N_{\text{dof}}]$ )
$\mathbf{M}(\tilde{p}_1, \dots, \tilde{p}_n)$	mass matrix depending on fuzzy parameters $\tilde{p}_1, \dots, \tilde{p}_n$ (size $[N_{\text{dof}} \times N_{\text{dof}}]$ )
$n$	number of fuzzy parameters
$n_d$	number of discrete values
$N_{\text{dof}}$	number of degrees of freedom
$p_c$	crisp value of fuzzy parameter $\tilde{p}$
$p_i$	design parameter $i$
$\tilde{p}_i$	fuzzy design parameter $i$
$\underline{p}^\alpha$	lower bound for $\alpha$ -level cut of fuzzy number $\tilde{p}$
$\bar{p}^\alpha$	upper bound for $\alpha$ -level cut of fuzzy number $\tilde{p}$
$\tilde{p}^\alpha$	$\alpha$ -level cut of fuzzy number $\tilde{p}$
$[\underline{p}^0, \bar{p}^0]$	support of fuzzy number $\tilde{p}$
$\alpha$	$\alpha$ -level cut $i$
$\Delta \underline{p}^\alpha$	lower variation for $\alpha$ -level cut of fuzzy number $\tilde{p}$
$\Delta \bar{p}^\alpha$	upper variation for $\alpha$ -level cut of fuzzy number $\tilde{p}$
$\tilde{\Lambda}$	fuzzy spectral matrix (size $[N_{\text{dof}} \times N_{\text{dof}}]$ )
$\mu_i$	degree of confidence $i$
$\Phi$	fuzzy modal basis (size $[N_{\text{dof}} \times N_{\text{dof}}]$ )

Zadeh's Extension Principle [8]. This method is simple to implement, but is too expensive for most practical finite element applications, for which the finite element models require several thousand degrees of freedom and have numerous fuzzy parameters. To avoid this drawback, many authors have proposed alternative methods. These methods can be divided into 2 main groups: those using a matrix formulation and those using a parametric formulation.

In the matrix formulation, first proposed by Valliappan [14], specific interval matrices are built for each  $\alpha$ -cut level (e.g., in modal analysis, the interval mass and stiffness matrices). The interval problem is then transformed into a first-order [15–17] or high-order [18,19] perturbed problem, and the solutions are obtained by calculating the interval bounds. These techniques, though less time consuming than the Extension principle, supply only an idea of the behaviour variation but do not provide the real variations needed in the design phase. More recently, the matrix formulation has been replaced by a parametric formulation, in which the interval problem is transformed into a discrete problem for each  $\alpha$ -cut level. The global strategy of this formulation is to look for combinations of discretized fuzzy design parameter values, which indicate the extreme variations for each  $\alpha$ -cut level. This strategy leads to a significant number of deterministic finite element simulations [20]. Obviously, the proposed methods provide a general idea of the behaviour variation, but not necessarily the most extreme variations. Among these methods, some are based on the strong assumption that a linear functional dependency is sufficient for assessing variability [21,22]. None of the methods deal with mode shape pairing or building eigenvector membership functions, which are generally not taken into account at all.

This paper introduces a new alternative to Zadeh's Extension Principle. The main goal of this alternative method is to calculate both fuzzy eigenvalues and fuzzy eigenvectors with a good level of precision and an acceptable CPU time. For the context described above, three fundamental notions are needed to efficiently compute the fuzzy solution sets, namely functional dependence, mode shape pairing and high-order approximations. Section 2 presents a brief overview of the formulation of fuzzy finite element modal analysis. In Section 3, the main characteristics of Zadeh's Extension Principle, which allows fuzzy numbers to be managed in a general context, are summarized. This principle was applied to solve fuzzy modal analysis problems in order to provide the reference data used in Section 6. Section 4 describes a parametric modal analysis method to highlight the mode shape pairing and functional dependence of the eigensolutions. In Section 5, these notions are used to explain the different steps of our method for calculating fuzzy modal solutions (eigenvalues and eigenvectors), and high-order approximations (i.e., Padé Approximants) are introduced to limit the computational cost associated with variability management. Our method, called PAEM (Padé Approximants with Extrema Management), is applied in Section 6 to several different test cases. The final section offers our conclusions and perspectives for future research.

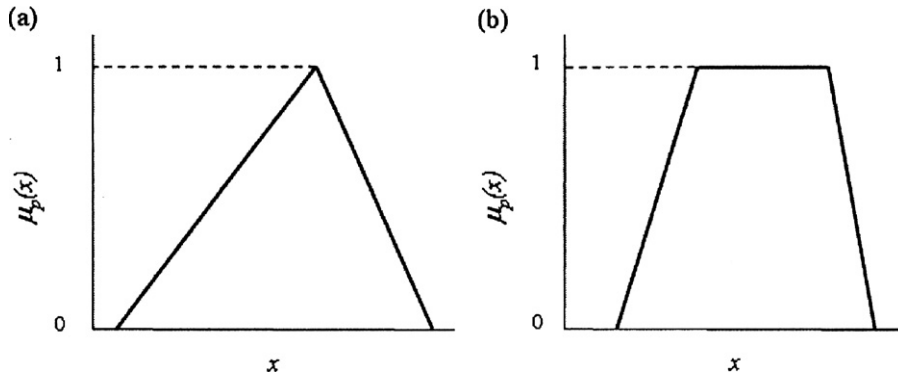


Fig. 1. Current forms of the membership functions: (a) triangular and (b) trapezoid.

### 2. Fuzzy modal approach

A variety of applications use a fuzzy set approach to describe non-deterministic data [8–12]. Fuzzy set theory is an extension of ordinary set theory, in which each object either belongs to a set or does not. Fuzzy set theory introduces the notion of degree of membership, using a membership function to describe, for each element in the domain, the level of membership in the fuzzy set. This function can take different forms, depending on the user’s perception of the input’s imprecision [14–16] and the kinds of imprecision considered. Fig. 1 presents the different forms of fuzzy numbers or fuzzy intervals  $\tilde{p}$  currently used. The membership function can also take other forms. In this article, the only restrictions are the normality and convexity of the fuzzy quantities. The fuzzy numbers are used to model the variability of the material properties or geometric characteristics of the finite element structure, such as Young’s modulus  $E$ , Poisson’s ratio  $\nu$ , density  $\rho$ , thickness  $e$  for shell elements, or section  $S$  for bar or beam elements. These parameters are considered to be independent and uniform.

With the fuzzy formalism, the eigenvalue problem which governs the modal analysis can be written as follows:

$$\mathbf{K}(\tilde{p}_1, \dots, \tilde{p}_n) \tilde{\Phi} = \mathbf{M}(\tilde{p}_1, \dots, \tilde{p}_n) \tilde{\Phi} \tilde{\Lambda}, \tag{1}$$

where

$$\tilde{\Phi}^T \mathbf{M}(\tilde{p}_1, \dots, \tilde{p}_n) \tilde{\Phi} = \tilde{\mathbf{I}} \tag{2}$$

and  $\mathbf{M}(\tilde{p}_1, \dots, \tilde{p}_n)$  and  $\mathbf{K}(\tilde{p}_1, \dots, \tilde{p}_n)$  are, respectively, the mass and stiffness matrices that are dependent on the fuzzy parameters  $\tilde{p}_1, \dots, \tilde{p}_n$ ,  $\tilde{\Phi}$  and  $\tilde{\Lambda}$  are, respectively, the fuzzy modal basis and fuzzy spectral matrix.

Fuzzy set theory has its own arithmetic, which allows the classic operations (e.g., +, −, ×) on the fuzzy scalars to be extended. Extending this arithmetic to problems with matrices or to other more complex problems (e.g., linear systems and eigenvalues) is not trivial and implies some overestimation. One solution described in fuzzy set theory is to use the Extension Principle developed by Zadeh.

### 3. Zadeh’s extension principle (ZEP)

Zadeh’s Extension Principle is outlined below:

Given a function  $\varphi$  that maps from  $X = X_1 \times X_2 \times \dots \times X_n$  to a universe  $Y$ , such that  $y = \varphi(x_1, x_2, \dots, x_n)$  where  $y \in Y$  and  $x_i \in X_i, \forall i$ , and considering the fuzzy subsets  $A_1, A_2, \dots, A_n$  defined for the reference sets  $X_1, X_2, \dots, X_n$ , the Extension Principle defines a fuzzy subset  $B$  of  $Y$  using the data from the fuzzy subsets  $A_1, A_2, \dots, A_n$  of  $X$ . A fuzzy characterization of the membership function in  $Y$  is written as follows:

$$\begin{aligned} \text{If } \varphi^{-1}(y) \neq \emptyset, \quad \mu_B(y) &= \sup \{ \min(\mu_{A_1}(x_1), \mu_{A_2}(x_2), \dots, \mu_{A_n}(x_n)) \}_{x \in X, y = \varphi(x)}, \\ \text{If } \varphi^{-1}(y) = \emptyset, \quad \mu_B(y) &= 0. \end{aligned} \tag{3}$$

In practice, this procedure is organized in three steps:

- Discretization of membership functions.  
Each membership function is discretized according to the support  $[\underline{p}^0; \bar{p}^0]$  (Fig. 2). The support is cut into  $n_d$  discrete values  $\{p_1, \dots, p_{n_d}\}$ , to which a degree of confidence  $\{\alpha_1, \dots, \alpha_{n_d}\}$  is associated. Fig. 3 presents this discretization step for two fuzzy parameters. The parameter variation domain (before discretization) is represented by the central square of the figure. The problem is of a continuous nature. After discretization, this problem is transformed by a discrete problem, in which the parameter variation domain is represented by all the possible combinations of discrete fuzzy parameter values. These combinations are represented by the circles in Fig. 3.
- Calculation of deterministic solutions due to all the combinations of values of fuzzy parameters.  
The strategy is to calculate all these combinations in order to determinate the minimum and maximum variations of the studied solutions.
- Evaluation of the degree of confidence of all the solutions.  
The membership functions of the solutions are built by considering that the degree of membership of one combination is equal to the smallest degree of membership of the independent parameters in this combination. In the case of multiple occurrences of a solution, the final membership degree is equal to the maximum membership degree of the different solutions.

The following example is used to illustrate the Extension Principle. Consider two fuzzy numbers  $\tilde{a}$  and  $\tilde{b}$ ; an application  $\varphi$ , defined as the operation “multiplication”; and the output fuzzy number  $\tilde{c}$  obtained by the Extension Principle (Fig. 3).

In Fig. 3, the degree of confidence of the fuzzy numbers  $\tilde{a}$  and  $\tilde{b}$  in case (1) is equal to 1 and 1/3, respectively. The degree of confidence for this combination is thus equal to the minimum degree (i.e., 1/3), and the calculation yields a value of 1. For case (2), the degree of confidence is 1/2, and the result of the calculation is also 1. Taken together, cases (1) and (2) produce a multiple occurrence of the solution: 1. The final degree of confidence for the combination is therefore equal to the maximum degree of confidence (i.e., 1/2).

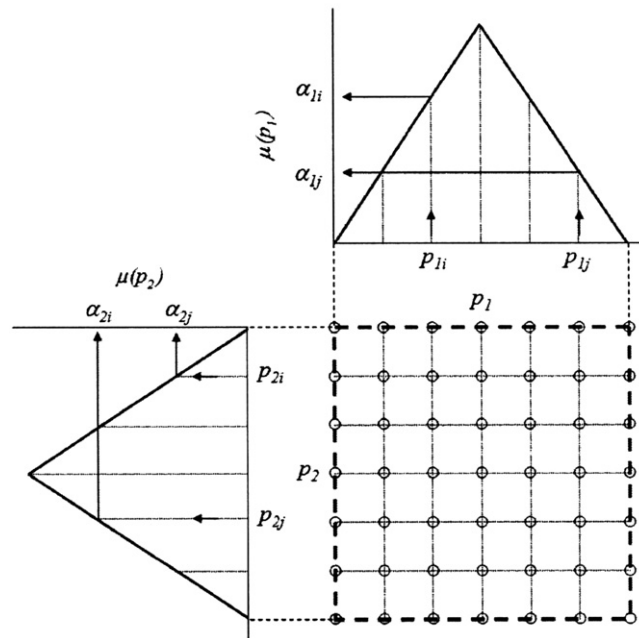


Fig. 2. Discretization of fuzzy numbers  $\tilde{p}_1$  and  $\tilde{p}_2$  according to the support: - - -, parameter variation domain and  $\circ$ , discrete parameter value combinations.

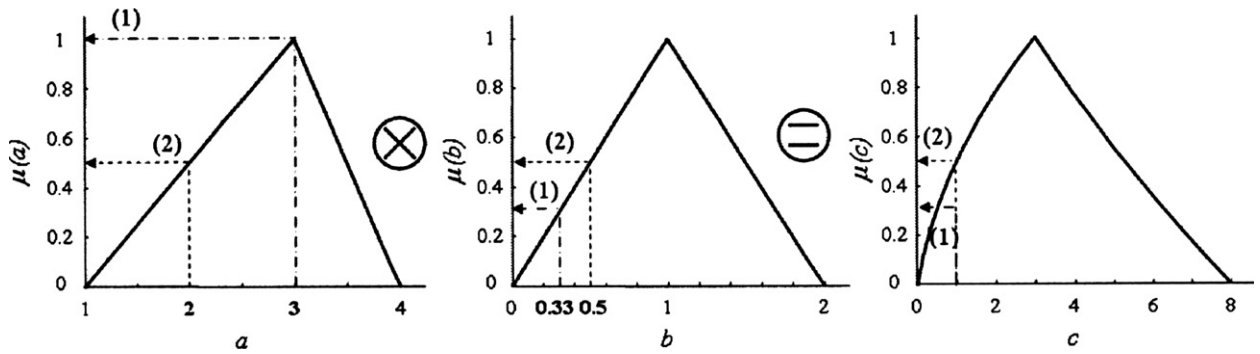


Fig. 3. An illustration of Zadeh's Extension Principle.

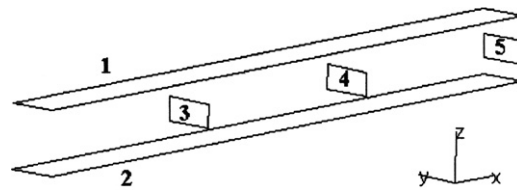


Fig. 4. A cantilever box beam.

This ZEP approach is very attractive because it is simple to implement. It defines a subset that characterizes all the variations of the solutions studied according to a specific application, such as an eigenvalue problem. However, when the size of the finite element model or the number of fuzzy parameters increases, this approach rapidly becomes too time consuming. For a study of two fuzzy parameters with 7 discretization values (Fig. 3), the representative set of the variation domain is defined by  $7^2$  values (49 values). Thus, for  $n$  fuzzy parameters, with  $n_d$  discretization values, the number of deterministic calculations will be  $n_d^n$ .

This ZEP method was applied to solve fuzzy modal analysis problems in order to provide the reference data that will allow us to compare and quantify the efficiency of our alternative method. These reference data are referred to in Section 6.

#### 4. Parametric modal analysis

In this section, a parametric analysis is defined and performed for one fuzzy parameter in order to show the functional dependence of the fuzzy eigensolutions and to facilitate the explanation of mode shape pairing. These two fundamental notions—functional dependence and mode shape pairing—govern behaviour variations in modal analysis. A numerical test case, presented in the next section, is used to illustrate the effect of these two notions on fuzzy eigensolutions. Though the analysis is performed for only 1 parameter, the proposed solutions can, of course, be applied in the case of multiple fuzzy parameter variations.

##### 4.1. Description of the test case

Consider the cantilevered box beam shown in Fig. 4. This structure is composed of 5 plates and modelled with 265 triangular shell elements and 1134 degrees of freedom (Fig. 5). Its material properties are: Young's modulus  $E = 72 \times 10^9 \text{ N/m}^2$ , Poisson's ratio  $\nu = 0.3$ , and density  $\rho = 2700 \text{ kg/m}^3$ . Its overall geometric characteristics are: length  $L = 3 \text{ m}$ , width  $l = 0.2 \text{ m}$ , and height  $h = 0.1 \text{ m}$ , with the individual plates  $e$  being 2 mm thick.

The first eight frequencies of the structure are presented in Table 1. These frequencies constitute the initial data for the parametric study. In order to simplify the discussion, the parametric study was performed only for a variation in the thickness of the third plate ( $e_3$ ), which varied from 1.6 to 2.6 mm. The fuzzy eigensolutions were evaluated using Zadeh's Extension Principle, where the fuzzy thickness  $\tilde{e}_3$  is represented by a triangular

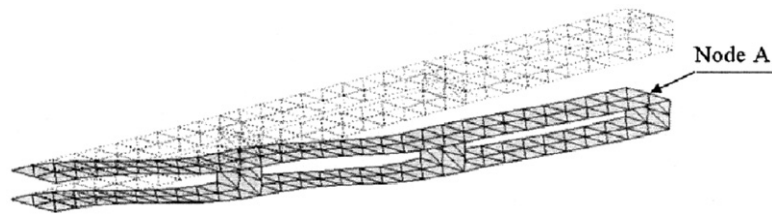


Fig. 5. A finite element model of the cantilever box beam.

Table 1  
First eight frequencies of the cantilevered box beam

	1	2	3	4	5	6	7	8
Frequencies (Hz)	0.80	2.47	4.09	8.77	9.75	10.51	10.71	13.61

fuzzy number defined by the lower bound (1.6 mm), the crisp value (2 mm) and the upper bound (2.6 mm). For the applications, the most standard form—the triangular one—was chosen to model the variability, which was defined solely with the data at our disposal, namely a nominal value and its extreme variations. In this case, the degree of confidence of the different eigensolutions can be directly deduced from the degree of confidence of the fuzzy thickness.

#### 4.2. Functional dependence of eigensolutions

Depending on the type of solutions studied (e.g., displacements, stresses, eigenvalues, eigenvectors) and the fuzzy parameters (e.g., Young's modulus, Poisson's ratio, density), the nature of functional dependence is not always the same. This dependence can be monotonic (e.g., linear, quadratic) or not.

For certain parameters, simple rules can be defined because the solutions' functional dependence is monotonic. For example, eigenvalues tend to increase as Young's modulus increases and decrease as density increases. However, for other parameters, such as Poisson's ratio or plate thickness, the functional dependence is not always monotonic, particularly given large variations. These parameters are present in both the mass and stiffness matrices, either defined by a rational fraction in the case of Poisson's ratio, or as a function of power in the case of plate thickness. For these kinds of parameters, the functional dependence is different for each eigenvalue and for each component of the solution vector. The study of the different applications shown in Fig. 6 highlights some extrema for a modal solution  $s_i$  (mainly for the case of eigenvectors).

Given this variation in the nature of the solutions' functional dependence, the hypothesis of linearity and monotonicity used by many authors [21,22] can thus imply errors in the calculation of the fuzzy solutions since the form of the membership function depends directly on the nature of the functional dependence (Fig. 7). In the non-monotonic case, certain parameter value combinations, which do not include all the fuzzy parameter bounds, are needed to characterize the solution subsets with precision. The search for these specific combinations is the first step of our method.

#### 4.3. Mode shape pairing

This section examines the effect of modifying the form of the mode shapes and shows that mode shape pairing can also affect fuzzy eigensolutions.

In modal analysis, the Modal Assurance Criterion (MAC) is usually calculated for the mode shape pairing prior to comparing frequencies. The MAC is obtained using the following equation:

$$\text{MAC}_{(\phi_1, \phi_2)} = \frac{\|\phi_1^T \phi_2\|^2}{(\phi_1^T \phi_1)(\phi_2^T \phi_2)}, \quad (4)$$

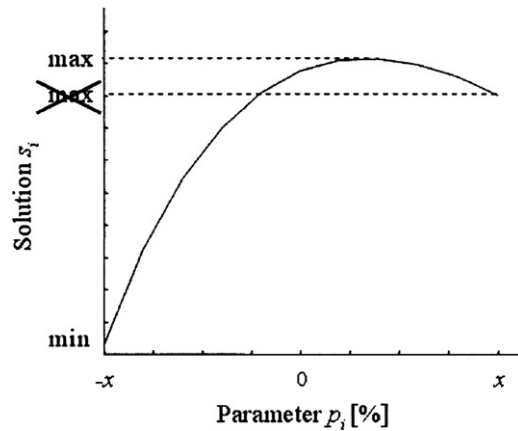


Fig. 6. Influence of extrema on the interval solution.

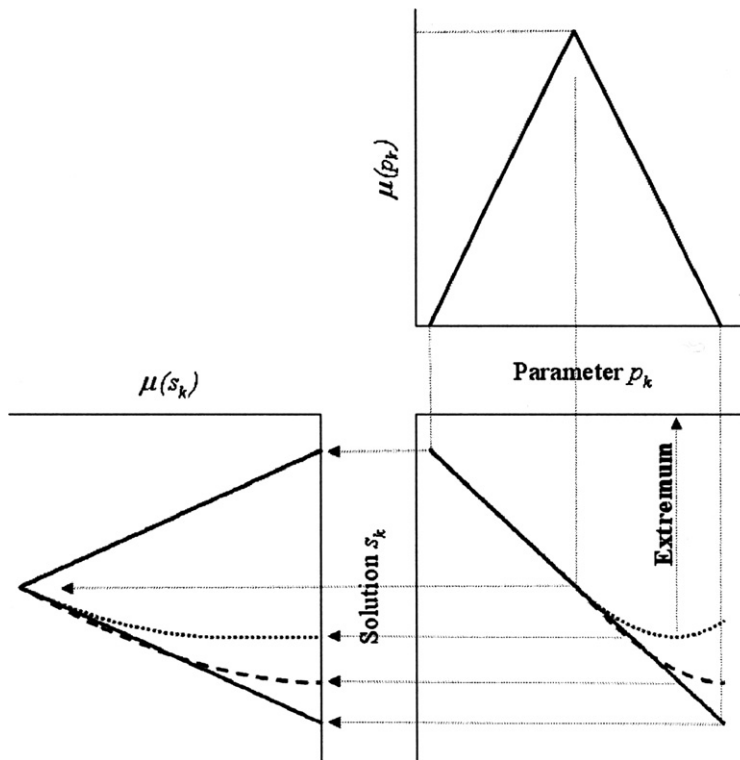


Fig. 7. Influence of nature of the function’s behaviour on the membership function: —, linear behaviour; - - -, quadratic behaviour; ·····, non-monotonic behaviour.

where  $\phi_1$  and  $\phi_2$  are two mode shapes to be compared. Generally, MAC values ranging from 0.8 or 0.9 to 1 are considered to define a good correlation between two mode shapes, especially for numerical data. Below this limit, notable differences can appear locally in the mode shape, leading to a permutation between frequencies.

Let us consider the 5th, 6th and 7th modes of the cantilever box beam. If certain parameters are varied, two situations arise:

- for certain frequencies, the associated mode shapes will always appear in the same order as the initial one (e.g., the 5th mode shape) and



- for other frequencies, the order of the mode shapes can change, whether or not the initial frequencies were distinct (e.g., the 6th and 7th mode shapes).

These situations are illustrated in Fig. 8, which shows the variation of the MAC based on a comparison of the mode shapes in the initial model ( $\phi_i$ ) with those in the modified models ( $\phi_m$ ). Fig. 9 shows the resulting fuzzy frequencies if the Extension Principle is applied without reorganizing the frequency subsets according to mode pairing. Clearly, the 6th and 7th fuzzy frequencies, as well as the fuzzy component of the eigenvectors, are wrong because the subsets solution aggregate mode shapes of different natures. In order to associate the modified eigenvectors with the initial ones for the same shapes, we propose to define a criterion based on a maximum MAC value. This criterion is traditionally used in experimental modal analysis to associate experimental mode shapes with numerical mode shapes before calculating the eigenfrequency error.

As shown in Fig. 8, this criterion can be successfully applied in most situations, except in the vicinity of  $e_3 = 2.4$  mm. For this specific zone, the criterion could be considered to be inadequate, since the MAC is very small, which indicates no pairing. This specific case is highlighted on curve (a) in Fig. 11, which corresponds to the maximum MAC values between the 6th and 7th modified eigenvectors and the 6th initial eigenvector. These small values are due to modifying only two mode shapes (from distinct modes to multiple modes and vice versa), which are always compared with the initial distinct mode shapes (Fig. 10). Thus, in spite of MAC values less than 0.9, the criterion still aggregates eigenvectors of the same type. Curve (b) in Fig. 11 is even more convincing; it represents the variation in the MAC criterion applied to the 6th eigenvectors for two consecutive  $e_3$  parameter values. The slight difference between the two values leads to a small change in the mode shapes, which can now be better compared.

The use of this MAC for fuzzy calculations implies reorganizing the frequencies and eigenvectors, which allows good quality membership functions to be obtained (Fig. 12). These deterministic eigenvectors are traditionally calculated via mass normalization. However, for fuzzy eigenvector aggregation, a unit norm is preferred in order to provide a better indication of variability. Thus, in this case, mass changes are not taken into account. Mode pairing and vector normalization will be applied in both the ZEP reference method and our PAEM method.

## 5. Padé Approximants with Extrema Management method (PAEM)

In this section, we introduce our new method for calculating fuzzy eigensolutions. This method is based on the fundamental notions described in Section 4, namely the functional dependence of eigensolutions and mode shape pairing.

Calculating with fuzzy numbers requires discretizing each membership function. The discrete fuzzy numbers are obtained from cuts, according to the degree of confidence (Fig. 13). The fuzzy problem is then transformed

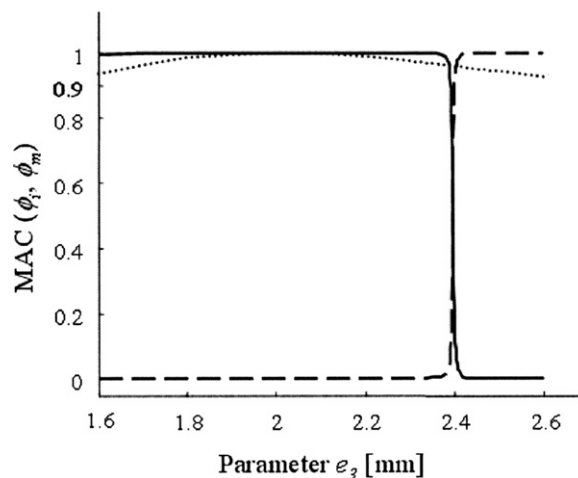


Fig. 8. MAC criterion for the 5th, 6th and 7th mode shapes:  $\cdots\cdots\cdots$ ,  $\text{MAC}(\phi_{5i}, \phi_{5m})$ ;  $\text{—}$ ,  $\text{MAC}(\phi_{6i}, \phi_{6m})$ ;  $\text{---}$ ,  $\text{MAC}(\phi_{6i}, \phi_{7m})$ .



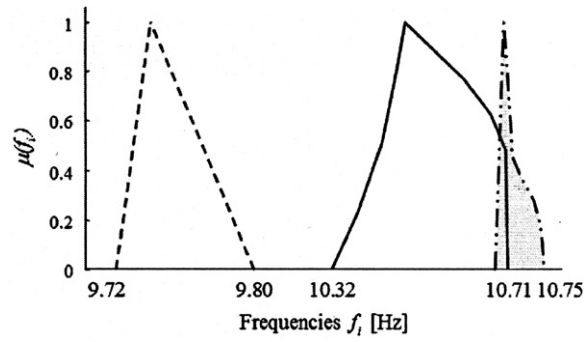


Fig. 9. Membership functions for frequencies 5–7 without mode pairing (obtained by ZEP): - - -, frequency  $f_5$ ; —, frequency  $f_6$ ; - · · -, frequency  $f_7$ .

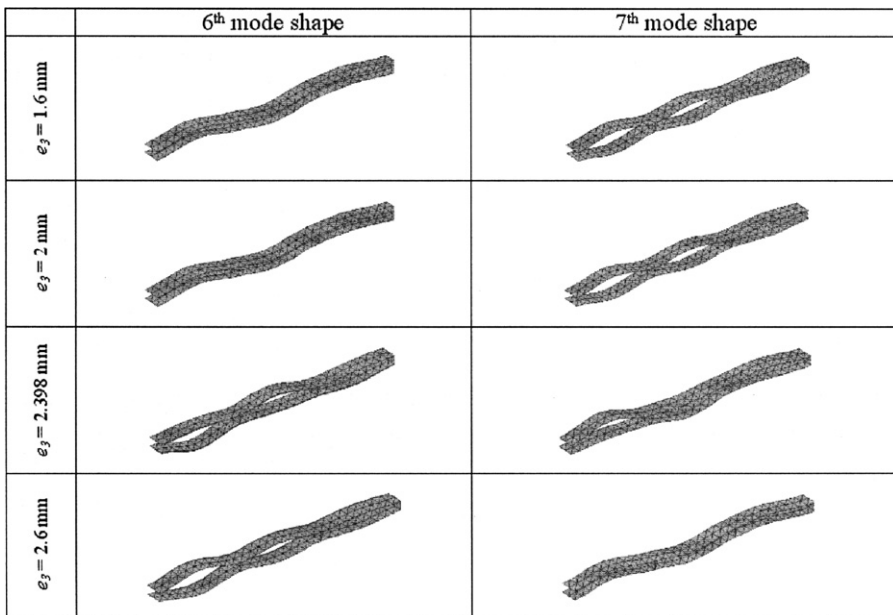


Fig. 10. Mode shape for different thickness values  $e_3$ .

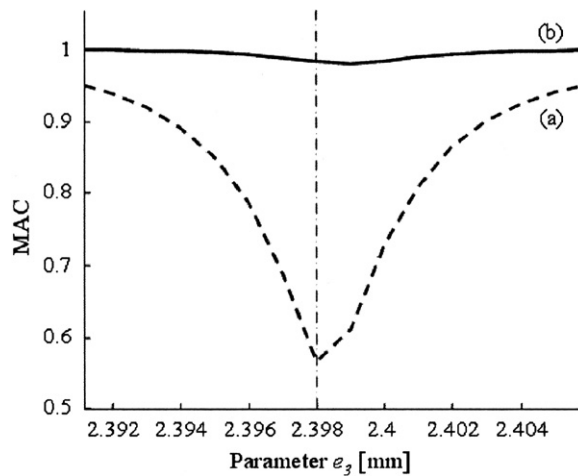


Fig. 11. MAC criterion: (a) - - -,  $\max(\text{MAC}(\phi_{6i}, \phi_{6m}) \text{ and } \text{MAC}(\phi_{6i}, \phi_{6m}))$  and (b) —,  $\text{MAC}(\phi_{6i}, \phi_{6m})$  for two consecutive values of  $e_3$ .

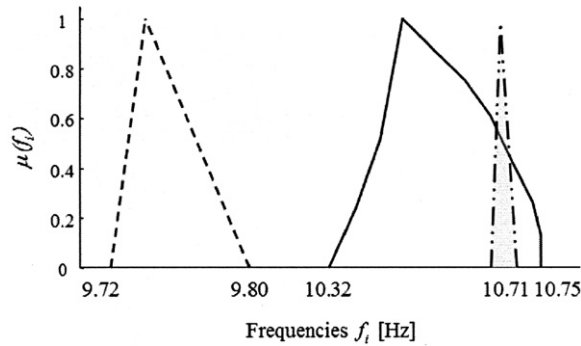


Fig. 12. Membership functions for frequencies 5–7 with mode pairing (obtained by ZEP - - -, frequency  $f_5$ ; —, frequency  $f_6$ ; - · · ·, frequency  $f_7$ ).

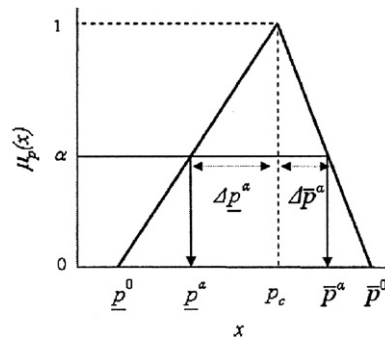


Fig. 13. Discretization of fuzzy number  $\tilde{p}$  according to the degree of confidence.

into a series of interval problems, each defined for a  $\alpha$ -cut level. For each  $\alpha$ -cut level, an interval  $\tilde{p}^\alpha$  is defined by the lower and upper bounds,  $\underline{p}^\alpha$  and  $\bar{p}^\alpha$  respectively, or by a crisp value  $p_c$  and two variations,  $\Delta \underline{p}^\alpha$  and  $\Delta \bar{p}^\alpha$ . This interval is expressed as follows:

$$\tilde{p}^\alpha = [\underline{p}^\alpha, \bar{p}^\alpha], \quad \tilde{p}^\alpha = [p_c - \Delta \underline{p}^\alpha; p_c + \Delta \bar{p}^\alpha]. \tag{5}$$

Following the example of the ZEP method, the parameter variation domain is also discretized and is represented by a set of discrete parameter value combinations for each  $\alpha$ -cut level. Unlike the ZEP method, in which all the parameter value combinations are evaluated, our strategy involves limiting the number of calculations for these combinations, thus limiting the additional cost due to variability management. Our method uses a sensitivity analysis [23,24] to detect the combinations of parameter values for each  $\alpha$ -cut level that will lead to the minimum and maximum eigensolution variations. This algorithm is presented in the following section.

### 5.1. The PAEM algorithm

The PAEM algorithm (Fig. 14) consists of the following steps:  
 For the crisp values ( $\alpha = 1$ ):

- Determine the modal quantities and their first sensitivities for each fuzzy parameter. The signs of the first-order sensitivities indicate the functional dependence of the response function and define the combinations of discrete fuzzy parameter values for the following  $\alpha$ -cut level, which could supply the minimum and maximum variations (Step 1).

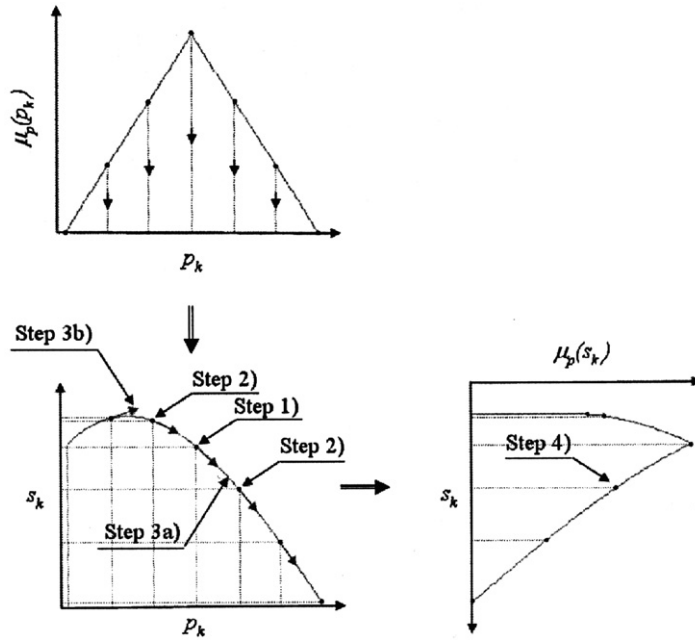


Fig. 14. Construction of fuzzy number solution  $\tilde{s}_k$ .

For each  $\alpha$ -cut level:

- Evaluate the first derivatives of the modal quantities for the combinations of discrete fuzzy parameter values determined at the previous  $\alpha$ -cut level (Step 2).
- Compare the signs of the derivatives with those obtained at the previous  $\alpha$ -cut level.
  - If the sensitivities have the same signs, the response function is considered to be locally monotonic, and the determined combinations provide the minimum and maximum variations of the modal quantities for the current  $\alpha$ -cut level (Step 3a).
  - If the sensitivities have different signs, the response function cannot be considered as monotonic, giving rise to an extremum between these two  $\alpha$ -cut levels. The combination nearest the extremum is chosen and the search is stopped for this variation (Step 3b).
- Calculate the eigensolutions for the selected combinations of discrete fuzzy parameter values and apply the MAC criterion to verify the form of the modes. To decrease the calculation time and maintain a good level of accuracy, the “exact” calculation (corresponding to a deterministic finite element simulation) can be replaced by a high-order approximation, using Padé rational functions [25–27], for example. This type of approximation is described in the next section.

### 5.2. High-order approximation

Let us consider the modified eigensolution vector  $\mathbf{U}_m$  of length  $N_{\text{dof}+1}$  defined by  $\begin{pmatrix} \phi_j^m \\ \lambda_j^m \end{pmatrix}$ , where  $\lambda_j^m$  and  $\phi_j^m$  represent the  $j$ th modified eigenvalue and eigenvector of the structure (the index  $j$  will be omitted in the next part).

The modified eigensolutions  $\mathbf{U}_m$  are therefore expressed as a series  $\mathbf{S}_n(\mathbf{U}_m(\varepsilon))$ , defined as

$$\mathbf{S}_n(\mathbf{U}_m(\varepsilon)) = \mathbf{U}_0 + \varepsilon\mathbf{U}_1 + \dots + \varepsilon^n\mathbf{U}_n. \tag{6}$$

This means that

$$\mathbf{S}_n \begin{pmatrix} \phi_m(\varepsilon) \\ \lambda_m(\varepsilon) \end{pmatrix} = \begin{pmatrix} \phi_0 \\ \lambda_0 \end{pmatrix} + \varepsilon \begin{pmatrix} \phi_1 \\ \lambda_1 \end{pmatrix} + \dots + \varepsilon^n \begin{pmatrix} \phi_n \\ \lambda_n \end{pmatrix}, \tag{7}$$

where  $\epsilon$  represents an additional unknown that allows the perturbed problem to be defined. This unknown is similar to the control parameter of classic iterative algorithms. At the end of the calculation of Eq. (10), this parameter is fixed to 1.

The modified mass and stiffness matrices  $\mathbf{M}_m$  and  $\mathbf{K}_m$  are, respectively defined using the initial matrices  $\mathbf{M}_0$  and  $\mathbf{K}_0$  and the perturbation matrices  $\Delta\mathbf{M}$  and  $\Delta\mathbf{K}$ . The equation for the modified eigenvalue problem is thus written as

$$(\mathbf{K}_0 + \epsilon\Delta\mathbf{K})(\phi_0 + \epsilon\phi_1 + \dots + \epsilon^n\phi_n) = (\lambda_0 + \epsilon\lambda_1 + \dots + \epsilon^n\lambda_n)(\mathbf{M}_0 + \epsilon\Delta\mathbf{M})(\phi_0 + \epsilon\phi_1 + \dots + \epsilon^n\phi_n). \tag{8}$$

The vectors  $(\mathbf{U}_i)_{i=0\dots n}$  are determined after identifying the different order terms using Lee’s method [28,29]. For each order, the equations are put together in a linear system:

$$\begin{aligned} &\mathbf{K}_0\phi_0 = \lambda_0\mathbf{M}_0\phi_0 \\ \begin{bmatrix} \mathbf{K}_0 - \lambda_0\mathbf{M}_0 & -\mathbf{M}_0\phi_0 \\ -\phi_0^T\mathbf{M}_0 & 0 \end{bmatrix} &\begin{Bmatrix} \phi_1 \\ \lambda_1 \end{Bmatrix} = \begin{bmatrix} -(\Delta\mathbf{K} - \lambda_0\Delta\mathbf{M})\phi_0 \\ 0.5\phi_0^T\Delta\mathbf{M}\phi_0 \end{bmatrix}, \\ \begin{bmatrix} \mathbf{K}_0 - \lambda_0\mathbf{M}_0 & -\mathbf{M}_0\phi_0 \\ -\phi_0^T\mathbf{M}_0 & 0 \end{bmatrix} &\begin{Bmatrix} \phi_2 \\ \lambda_2 \end{Bmatrix} = \begin{bmatrix} -(\Delta\mathbf{K}\phi_1 - \lambda_0\Delta\mathbf{M}\phi_1 - \lambda_1\Delta\mathbf{M}\phi_0 - \lambda_1\mathbf{M}_0\phi_1) \\ 0.5(\phi_0^T\Delta\mathbf{M}\phi_1 + \phi_1^T\Delta\mathbf{M}\phi_0 + \phi_1^T\mathbf{M}_0\phi_1) \end{bmatrix}, \\ &\vdots \qquad \qquad \qquad \vdots \qquad \qquad \qquad \vdots \\ \begin{bmatrix} \mathbf{K}_0 - \lambda_0\mathbf{M}_0 & -\mathbf{M}_0\phi_0 \\ -\phi_0^T\mathbf{M}_0 & 0 \end{bmatrix} &\begin{Bmatrix} \phi_n \\ \lambda_n \end{Bmatrix} = \begin{bmatrix} -\left(\Delta\mathbf{K}\phi_{n-1} - \sum_{k=0}^{n-1} \lambda_k\Delta\mathbf{M}\phi_{n-k-1} - \sum_{k=1}^{n-1} \lambda_k\mathbf{M}_0\phi_{n-k}\right) \\ 0.5\left(\sum_{k=0}^{n-1} \phi_k^T\Delta\mathbf{M}\phi_{n-k-1} + \sum_{k=1}^{n-1} \phi_k^T\mathbf{M}_0\phi_{n-k}\right) \end{bmatrix}. \end{aligned} \tag{9}$$

The results obtained with Eq. (6) are equivalent to those obtained with the Neumann series [19]. However, as soon as the variations associated with the parameters become significant, the convergence of the Neumann approximation cannot be guaranteed. In order to avoid this limitation of the Neumann approximations, our method uses Pad e approximants, thus extending the domain of convergence and improving the precision of the approximations.

In order to illustrate the Pad e approximation [30] process, let us consider the function  $f(x) = \sqrt{\frac{1+1/2x}{1+2x}}$ . This function can be approximated using either a MacLaurin series  $f(\epsilon) = 1 - 3/4x + 39/32x^2 + O(x^3)$ , or a rational fraction  $f(\epsilon) = \frac{1+7/8x}{1+13/8x} + O(x^3)$  (Fig. 15). The MacLaurin series has a convergence radius equal to 1/2 and thus diverges when  $\epsilon$  is superior to 1/2. The rational fraction approximation, on the other hand, is remarkably accurate throughout the entire interval studied.

Taking these considerations into account, the series  $\mathbf{S}_n(\mathbf{U}_m(\epsilon))$  is replaced by a rational fraction  $\mathbf{F}_n(\mathbf{U}_m(\epsilon))$ :

$$\mathbf{F}_n(\mathbf{U}_m(\epsilon)) = \mathbf{U}_0 + \epsilon \frac{D_{n-2}(\epsilon)}{D_{n-1}(\epsilon)} \mathbf{U}_1 + \dots + \epsilon^{n-1} \frac{D_0(\epsilon)}{D_{n-1}(\epsilon)} \mathbf{U}_{n-1}, \tag{10}$$

where  $(D_i(\epsilon))_{i=0\dots n-1}$ , are polynomials of degree  $i$  with real coefficients  $d_i$ , such as  $D_i(\epsilon) = d_0 + \epsilon d_1 + \epsilon^2 d_2 + \dots + \epsilon^i d_i$ .

In this case, since the studied quantities are vectors, two solutions are possible. Either each component of  $\mathbf{U}_i$  is considered to be independent [30], or each component is treated as a unique quantity [31], which produces better results. In the second possible solution, an orthonormal basis  $\mathbf{U}_i^*$  is defined from the vectors  $\mathbf{U}_i$ , such that  $\mathbf{U}_i = \sum_{j=1}^i \alpha_{ij} \mathbf{U}_i^*$ . The coefficients  $\alpha_{ij}$  are used to determine the coefficients  $d_i$  of  $D_i(\epsilon)$  and are calculated using an iterative Gram-Schmidt algorithm [32]. (More details about the coefficient calculations are provided in the Appendix and in Refs. [31–33].)

The precision of fuzzy modal solutions necessarily depends on the order of the Pad e approximants. To control the error in the Pad e approximation when there is no reference value, a criterion based on the difference between the approximated solutions for two successive orders of approximation  $p$  can be defined.

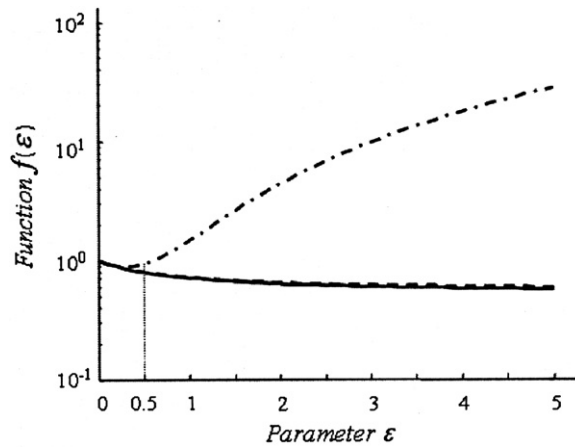


Fig. 15. Plot of the function  $f$  and these approximations: —, function  $f$ ; - · ·, MacLaurin approximation; - - -, rational approximation.

In the case of the eigenvalue, this criterion  $\widehat{\varepsilon}_\lambda$  is defined as follows:

$$\widehat{\varepsilon}_\lambda = \frac{\|\lambda_j(p)\| - \|\lambda_j(p + 1)\|}{\|\lambda_j(p)\|} \tag{11}$$

This  $\widehat{\varepsilon}_\lambda$  criterion allows the convergence of the Padé approximation and the precision of approximated solution to be verified. Please note that the eigenvalue problems presented in this paper require a third-order approximation to produce good results.

In the next section, the results of the PAEM method on a numerical test case are compared to the results of the ZEP method.

## 6. Numerical application

This section presents the results of the PAEM method for four test cases, thus demonstrating the efficiency of the method.

### 6.1. First test case

In order to obtain the same description of the eigensolution membership functions, the fuzzy parameters are defined using 6  $\alpha$ -cut levels for the PAEM method and 11 discrete values for the ZEP method. For these test cases, a third-order approximation was selected for the PAEM method.

The structure described in Section 4 was defined using fuzzy parameters. First, a triangular fuzzy number was defined to model the plate thickness  $e_3$ . Three sets of lower and upper bounds were fixed: [1.9–2.1 mm], [1.6–2.4 mm] and [1.6–4 mm]. The variation of the third frequency  $f_3$  in terms of the parameter  $e_3$  is presented in Fig. 16.

Fig. 17 presents a comparison of the  $\tilde{f}_3$  membership functions obtained with PAEM and ZEP for the different variation intervals. The results from PAEM are almost equal to those obtained by ZEP for all types of behaviour (i.e., linear, quadratic and non-monotonic). The maximal error is on the order of  $10^{-4}$  (Fig. 18). The results for this first case demonstrate the robustness of our method in terms of the nature of the solutions' functional dependence.

### 6.2. Second test case

In this second test case, a 20% variation in plate thickness was considered. Five fuzzy parameters were defined, and the first eight frequencies and mode shapes of the structure were determined.

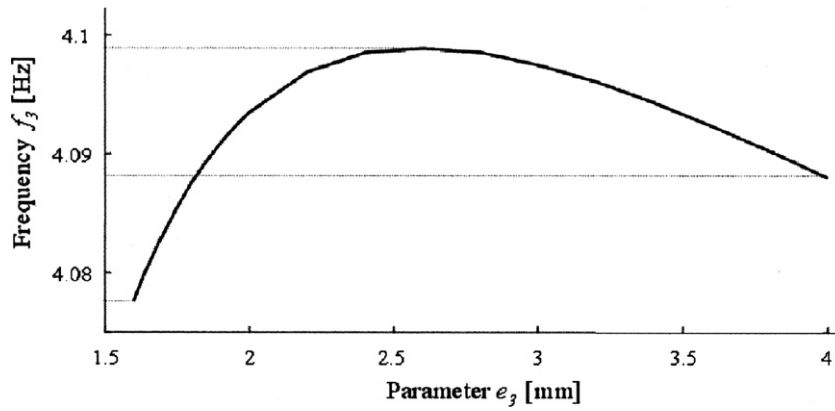


Fig. 16. Frequency  $f_3$  according to parameter  $e_3$ .

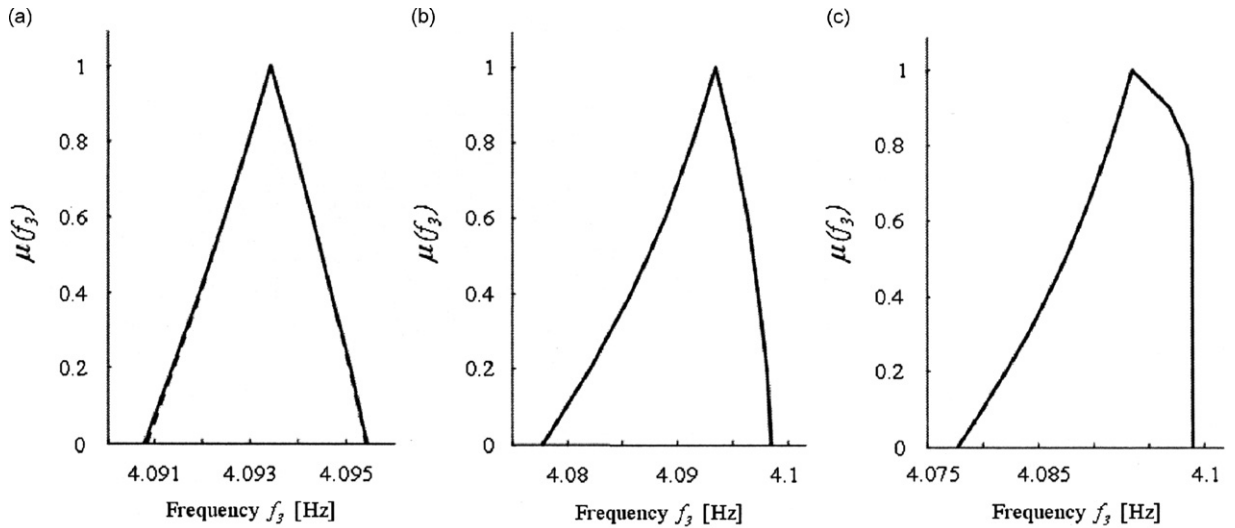


Fig. 17. Membership functions of  $\tilde{f}_3$  for the different variation intervals: (a) linear behaviour; (b) quadratic behaviour; (c) non-monotonic behaviour.

To further quantify how similar two correlated mode shapes might be, two scaled vector errors were defined as follows:

$$\text{err}_N(\%) = \frac{\left| \|\phi_1\| - \|\phi_2\| \right|}{\|\phi_1\|} \text{ to provide a global overview,} \quad (12)$$

$$\text{err}_{RN}(\%) = \frac{\|\phi_1 - \phi_2\|}{\|\phi_1\|} \text{ to highlight local errors,} \quad (13)$$

where  $\|\cdot\|$  is the Euclidian norm. The error corresponding to the lower and upper bounds for the frequencies and mode shapes, respectively, are shown in Figs. 19 and 20.

The results obtained with PAEM are very close to the reference data obtained with ZEP; the maximum error in the calculations of the lower and upper modal quantities was on the order of 5%. Figs. 21 and 22 clearly show the high level of accuracy of the eigenvalue membership functions and the mode shape predictions; the mapping represents the imprecision of the range of fuzzy eigenvectors.

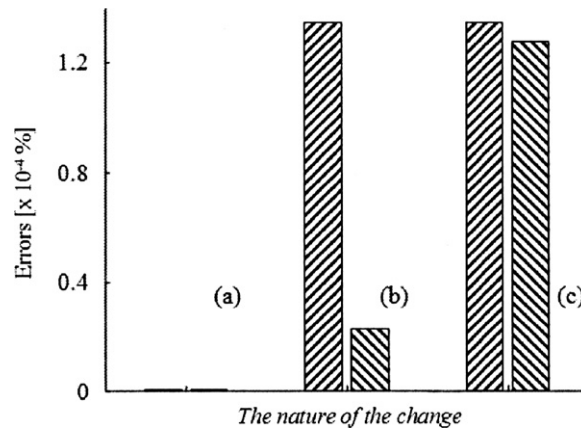


Fig. 18. Comparison of the lower and upper frequency errors produced by PAEM and ZEP for  $\alpha = 0$ : (a) linear behaviour, (b) quadratic behaviour and (c) non-monotonic behaviour. ▨, lower bounds and ▩, upper bounds.

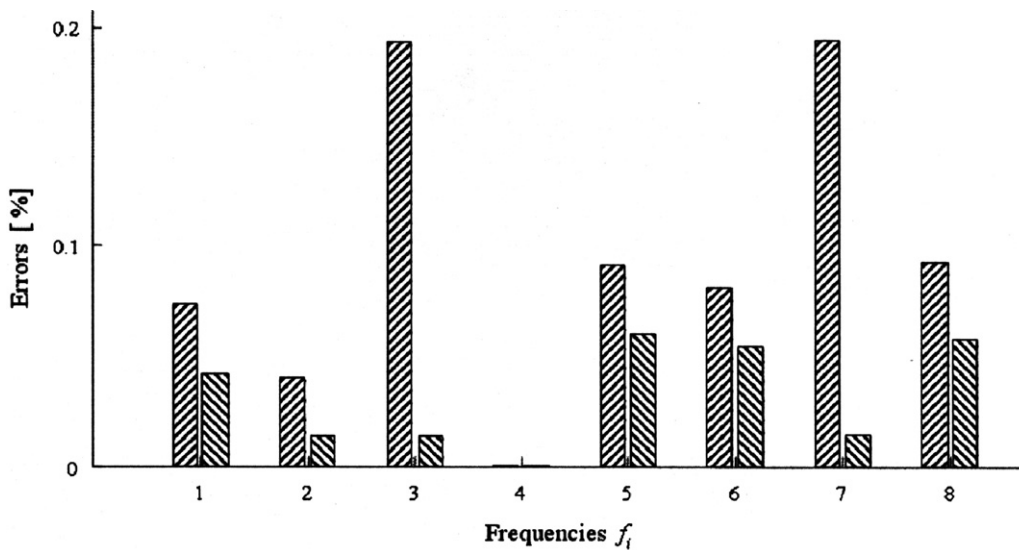


Fig. 19. Comparison of the lower and upper frequency errors produced by PAEM and ZEP for  $\alpha = 0$ . ▨, lower bounds and ▩, upper bounds.

For this test case, the combinatorial ZEP approach required the equivalent of  $5 \times 10^4$  deterministic calculations, whereas our method required only  $2 \times 10^3$  (Fig. 23). Thus, the PAEM requires less computing time than the ZEP method but yields very interesting results.

### 6.3. Third test case

To highlight the capabilities of our PAEM method, we tested it on an application with 15 independent fuzzy parameters of different natures. Variability was introduced in 10% of the nominal values for each plate for Young’s modulus, density and thickness. The fuzzy simulation was performed with the 15 fuzzy parameters discretized by 6  $\alpha$ -cut levels. This test was performed for the first eight frequencies and a specific component (degree of freedom 1107) of each mode shape (displacement following the Z-axis of Node A, as shown in Fig. 5).

Because this third test took 15 fuzzy parameters into account, the ZEP method could not be applied because it would have had to perform  $11^{15}$  deterministic finite element simulations, which would have required



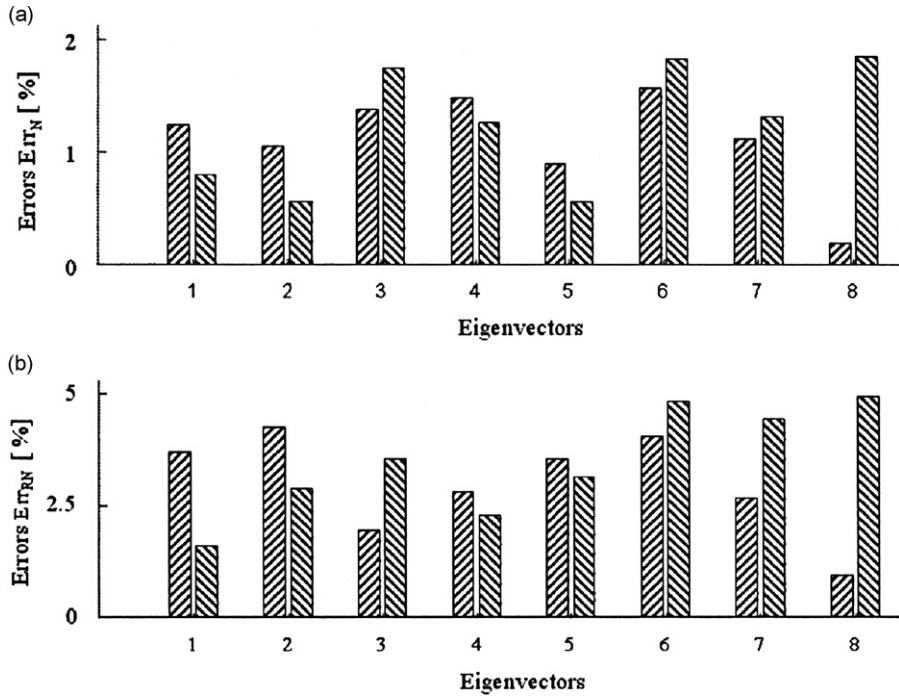


Fig. 20. Comparison of the lower and upper mode shapes produced by PAEM and ZEP for  $\alpha = 0$ : (a) errors Err<sub>N</sub> and (b) errors Err<sub>RN</sub>. ▨ lower bounds and ▩ upper bounds.

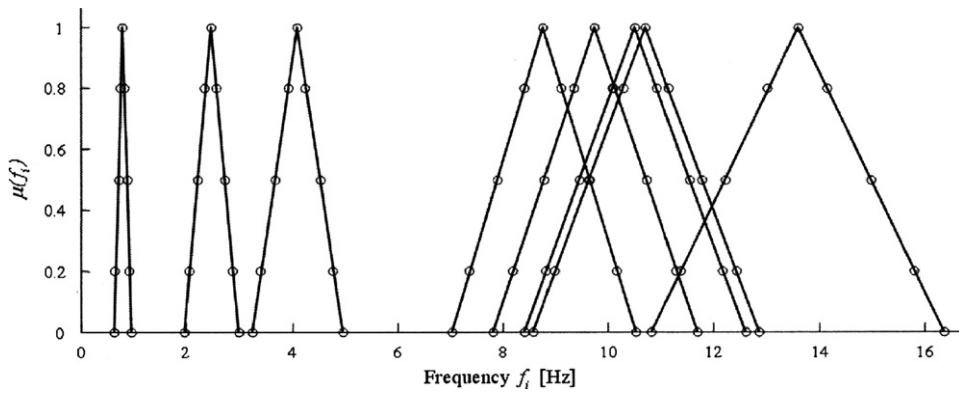


Fig. 21. Fuzzy frequency spectrum: —, ZEP method and —○—, PAEM method.

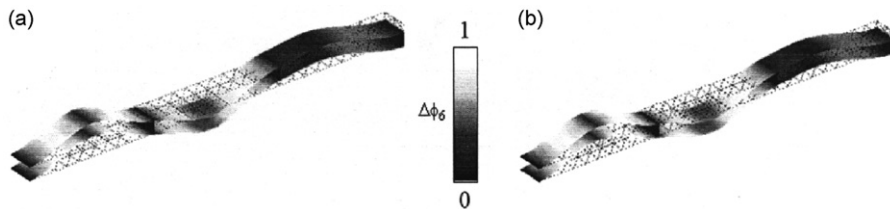


Fig. 22. Presentation of 6th mode shapes: (a) PAEM method and (b) ZEP method.

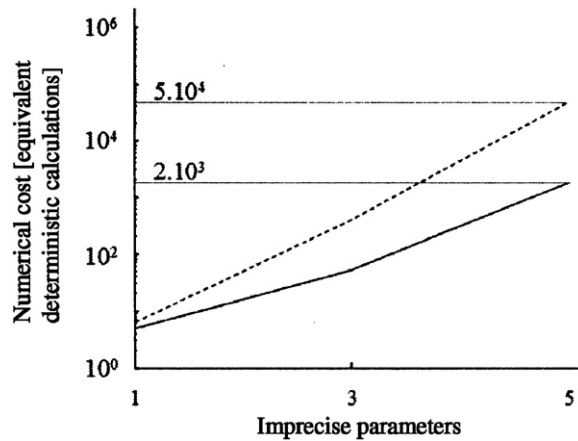


Fig. 23. Comparison of computing times: - - -, ZEP method and —, PAEM method.

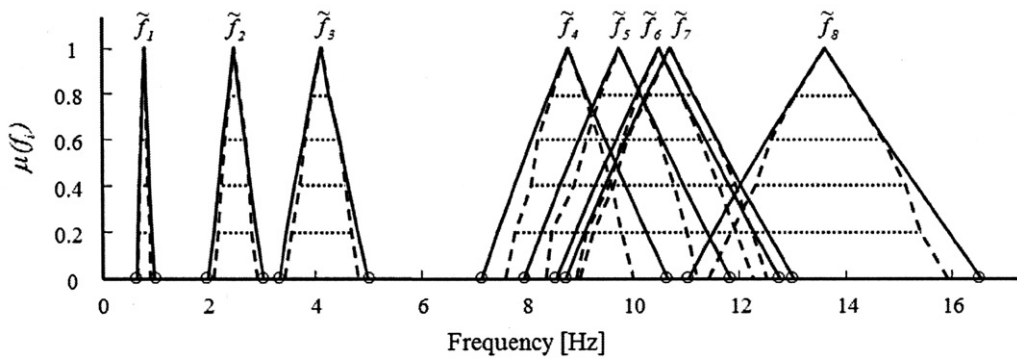


Fig. 24. Fuzzy spectrum of frequencies: —, PAEM method; - - -, random sampling; ·····, deterministic simulation; ○, exact calculations.

unrealistic amounts of CPU time. In order to partially prove the validity of the membership functions, two comparisons were made:

First, a random sampling was done amongst the 11<sup>15</sup> parameter value combinations in order to confirm that the membership functions calculated with PAEM included the calculated solutions. The number of samples was voluntarily limited to 50,000 to insure acceptable computational costs. This sampling procedure allowed us to verify that none of the samples produced a more extreme variation than the PAEM method.

Second, the approximated solution and the finite element solution were compared in terms of the quality of the Padé approximants for the parameter value combinations leading to extreme solution variations ( $\alpha = 0$ ).

The fuzzy spectrum of the eight tested frequencies is presented in Fig. 24. Results from the above two comparisons for the fourth eigenfrequency and component 1107 of the fourth mode shape are presented in Fig. 25. Table 2 lists the useful parameter value combinations mentioned above. Although the number of fuzzy parameters is significant, the results of PAEM method are quite satisfactory. The membership functions calculated with PAEM effectively include almost all the solutions obtained by the 50,000 finite element simulations. Moreover, the maximal errors made in the membership function support evaluations are less than 0.1% for the frequencies and less than 2% for the component of mode shapes, respectively. The random sampling was completed in 5 h and the PAEM calculations in 5 min. For the crisp values of the membership functions, no specific verification is necessary because these values are already calculated in the PAEM method using a finite element.

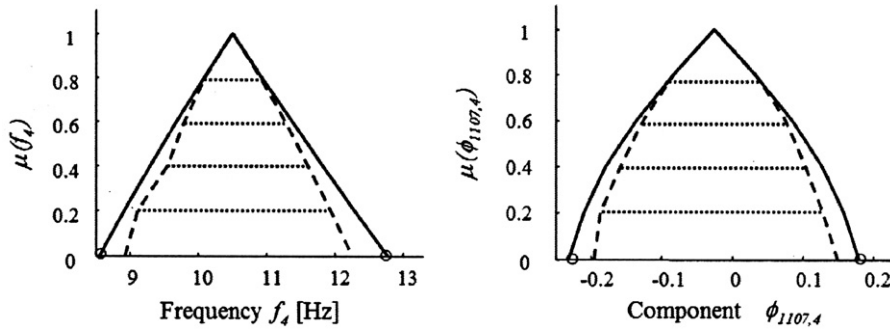


Fig. 25. Membership functions of  $\tilde{f}_4$  and  $\tilde{\phi}_{1107,4}$ : —, PAEM method; - - -, random sampling; ·····, deterministic simulation; ○, exact calculations.

Table 2  
Combinations of parameter values for third test case

	$f_1$ (Hz)	$f_2$	$f_3$	$f_4$	$f_5$	$f_6$	$f_7$	$f_8$	$\phi_{1107,4}$
Lower bound ( $\alpha = 0$ )									
$E_1$ (N m <sup>-2</sup> )	$6.48 \times 10^{10}$	$6.48 \times 10^{10}$	$6.48 \times 10^{10}$	$6.48 \times 10^{10}$	$6.48 \times 10^{10}$	$6.48 \times 10^{10}$	$6.48 \times 10^{10}$	$6.48 \times 10^{10}$	$6.48 \times 10^{10}$
$E_2$	$6.48 \times 10^{10}$	$6.48 \times 10^{10}$	$6.48 \times 10^{10}$	$6.48 \times 10^{10}$	$6.48 \times 10^{10}$	$6.48 \times 10^{10}$	$6.48 \times 10^{10}$	$6.48 \times 10^{10}$	$6.48 \times 10^{10}$
$E_3$	$6.48 \times 10^{10}$	$6.48 \times 10^{10}$	$6.48 \times 10^{10}$	$6.48 \times 10^{10}$	$6.48 \times 10^{10}$	$6.48 \times 10^{10}$	$6.48 \times 10^{10}$	$6.48 \times 10^{10}$	$7.92 \times 10^{10}$
$E_4$	$6.48 \times 10^{10}$	$6.48 \times 10^{10}$	$6.48 \times 10^{10}$	$6.48 \times 10^{10}$	$6.48 \times 10^{10}$	$6.48 \times 10^{10}$	$6.48 \times 10^{10}$	$6.48 \times 10^{10}$	$6.48 \times 10^{10}$
$E_5$	$6.48 \times 10^{10}$	$6.48 \times 10^{10}$	$6.48 \times 10^{10}$	$6.48 \times 10^{10}$	$6.48 \times 10^{10}$	$6.48 \times 10^{10}$	$6.48 \times 10^{10}$	$6.48 \times 10^{10}$	$7.92 \times 10^{10}$
$\rho_1$ (kg m <sup>-3</sup> )	2970	2970	2970	2970	2970	2970	2970	2970	2970
$\rho_2$	2970	2970	2970	2970	2970	2970	2970	2970	2970
$\rho_3$	2970	2970	2970	2970	2970	2970	2970	2970	2970
$\rho_4$	2970	2970	2970	2970	2970	2970	2970	2970	2430
$\rho_5$	2970	2970	2970	2970	2970	2970	2970	2970	2430
$e_1$ (m)	0.0018	0.0018	0.0018	0.0018	0.0018	0.0018	0.0018	0.0018	0.0018
$e_2$	0.0018	0.0022	0.0018	0.0018	0.0018	0.0018	0.0018	0.0022	0.0018
$e_3$	0.0018	0.0018	0.0022	0.0018	0.0018	0.0018	0.0018	0.0018	0.0022
$e_4$	0.0022	0.0022	0.0018	0.0018	0.0018	0.0018	0.0018	0.0018	0.0018
$e_5$	0.0018	0.0018	0.0018	0.0018	0.0018	0.0018	0.0018	0.0018	0.0022
Upper bound ( $\alpha = 0$ )									
$E_1$ (N m <sup>-2</sup> )	$7.92 \times 10^{10}$	$7.92 \times 10^{10}$	$7.92 \times 10^{10}$	$7.92 \times 10^{10}$	$7.92 \times 10^{10}$	$7.92 \times 10^{10}$	$7.92 \times 10^{10}$	$7.92 \times 10^{10}$	$7.92 \times 10^{10}$
$E_2$	$7.92 \times 10^{10}$	$7.92 \times 10^{10}$	$7.92 \times 10^{10}$	$7.92 \times 10^{10}$	$7.92 \times 10^{10}$	$7.92 \times 10^{10}$	$7.92 \times 10^{10}$	$7.92 \times 10^{10}$	$7.92 \times 10^{10}$
$E_3$	$7.92 \times 10^{10}$	$7.92 \times 10^{10}$	$7.92 \times 10^{10}$	$7.92 \times 10^{10}$	$7.92 \times 10^{10}$	$7.92 \times 10^{10}$	$7.92 \times 10^{10}$	$7.92 \times 10^{10}$	$6.48 \times 10^{10}$
$E_4$	$7.92 \times 10^{10}$	$7.92 \times 10^{10}$	$7.92 \times 10^{10}$	$7.92 \times 10^{10}$	$7.92 \times 10^{10}$	$7.92 \times 10^{10}$	$7.92 \times 10^{10}$	$7.92 \times 10^{10}$	$7.92 \times 10^{10}$
$E_5$	$7.92 \times 10^{10}$	$7.92 \times 10^{10}$	$7.92 \times 10^{10}$	$7.92 \times 10^{10}$	$7.92 \times 10^{10}$	$7.92 \times 10^{10}$	$7.92 \times 10^{10}$	$7.92 \times 10^{10}$	$6.48 \times 10^{10}$
$\rho_1$ (kg m <sup>-3</sup> )	2430	2430	2430	2430	2430	2430	2430	2430	2430
$\rho_2$	2430	2430	2430	2430	2430	2430	2430	2430	2430
$\rho_3$	2430	2430	2430	2430	2430	2430	2430	2430	2430
$\rho_4$	2430	2430	2430	2430	2430	2430	2430	2430	2970
$\rho_5$	2430	2430	2430	2430	2430	2430	2430	2430	2970
$e_1$ (m)	0.0022	0.0022	0.0022	0.0022	0.0022	0.0022	0.0022	0.0022	0.0022
$e_2$	0.0022	0.0018	0.0022	0.0022	0.0022	0.0022	0.0022	0.0018	0.0022
$e_3$	0.0022	0.0022	0.0018	0.0022	0.0022	0.0022	0.0022	0.0022	0.0018
$e_4$	0.0018	0.0018	0.0022	0.0022	0.0022	0.0022	0.0022	0.0018	0.0022
$e_5$	0.0022	0.0022	0.0022	0.0022	0.0022	0.0022	0.0022	0.0022	0.0018

6.4. Fourth test case

The aim of this last test was to show that, if only few specific fuzzy solutions are studied, the proposed method can be successfully applied in the case of multiple fuzzy parameters and a large industrial finite

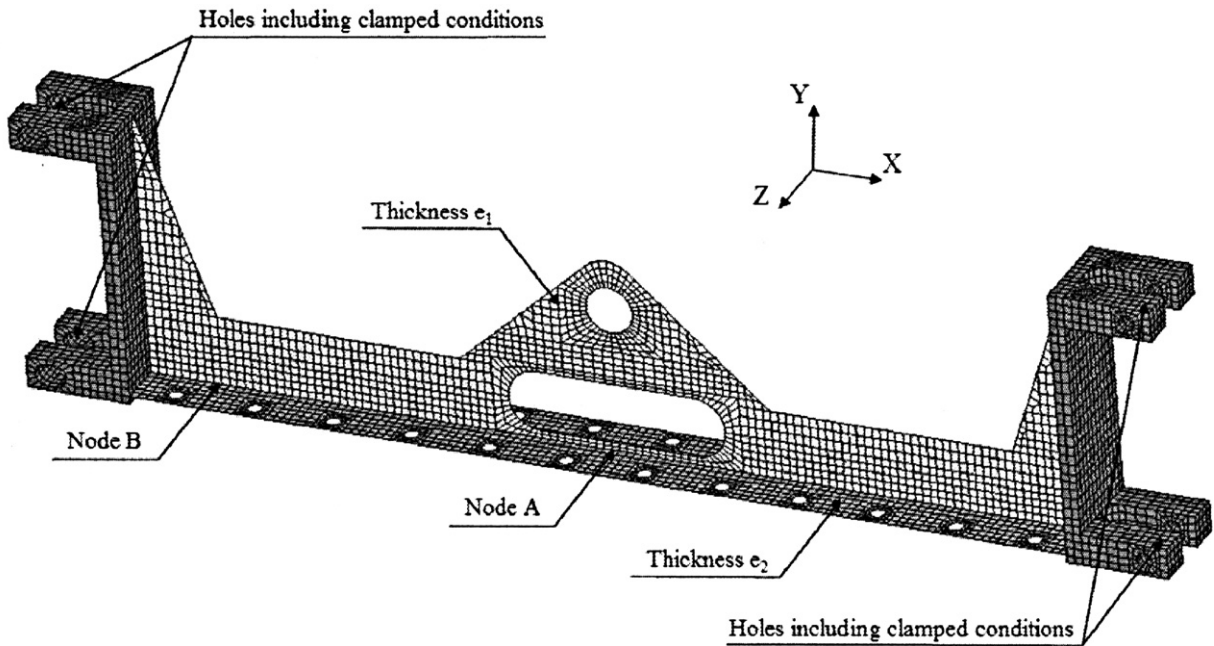


Fig. 26. Finite element model of the impactor sled.

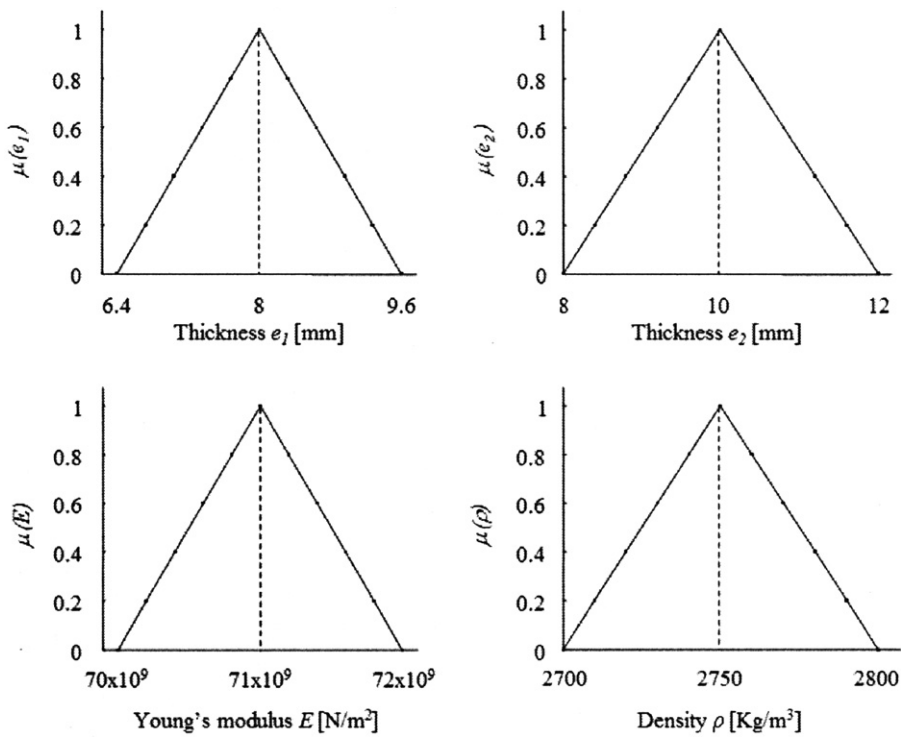


Fig. 27. Description of fuzzy parameters  $e_1$ ,  $e_2$ ,  $E$  and  $\rho$ .

element model. The test case was conducted on a drop tower impactor sled currently used for dynamic compression and bending tests. The finite element model (Fig. 26) used for the simulation contained 37,962 degrees of freedom (shell and brick elements). Clamped conditions were applied to eight holes.

Variability was introduced in 20% of the nominal thickness values for each plate in order to test the behaviour variation in terms of these parameters. Because the plate material was standard aluminium, for which no other information is known, variability was introduced into the Young’s modulus and density values in order to represent the entire variation interval [34]. These four parameters, presented in Fig. 27, were defined with triangular fuzzy numbers.

The two comparisons described in Section 6.3 were again performed in order to quantify the validity of PAEM method for this large finite element model. The results for the first eigenfrequency and components 4808 and 7640 of the first mode shape (following the axis  $Y$  of Nodes A and B, respectively, as shown in Fig. 26) are presented in Fig. 28. The number of simulations for the random sampling was limited to 1000. As in the third test case, the PAEM results are very interesting. The membership functions calculated with PAEM include the solutions of the finite element simulations. The maximal errors made on the membership function support evaluations (Table 3) are less than 4%, and the CPU time for the PAEM simulation was 5 mn.

Given the results from the 4 test cases, the PAEM method appears to be a general and efficient way to find solutions in fuzzy modal analysis. This method can be applied in cases involving multiple fuzzy parameters,

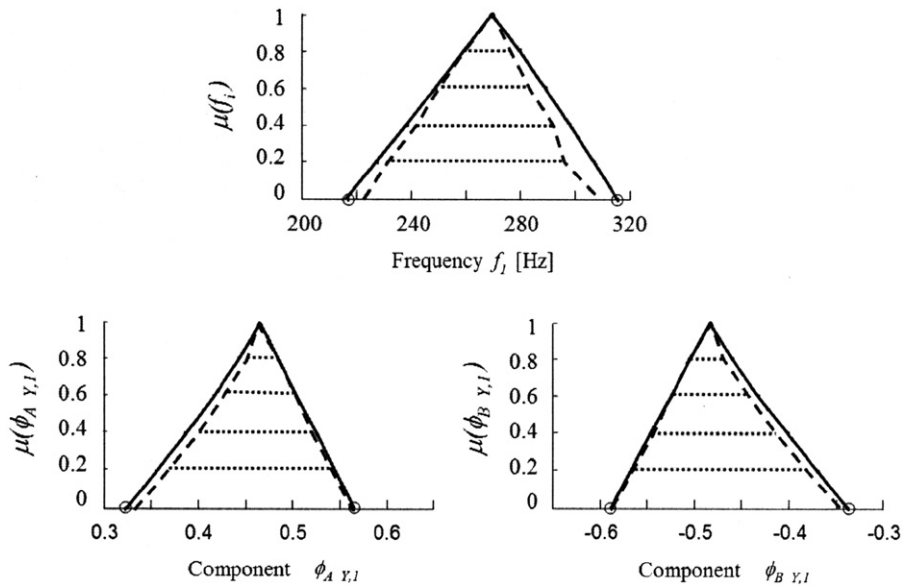


Fig. 28. Membership functions of  $\tilde{f}_1$ ,  $\tilde{\phi}_{AY,1}$  and  $\tilde{\phi}_{BY,1}$ : —, PAEM method; - - -, random sampling; ·····, deterministic simulation; ○, exact calculations.

Table 3  
Combinations of parameter values for fourth test case

	$E$ (Nm <sup>-2</sup> )	$\rho$ (kg m <sup>-3</sup> )	$e_1$ (m)	$e_2$ (m)
Lower bound ( $\alpha = 0$ )				
$f_i$ (Hz)	$7 \times 10^{10}$	2800	0.008	0.0064
$\phi_{4808,1}$	$7.2 \times 10^{10}$	2800	0.012	0.0064
$\phi_{7640,1}$	$7 \times 10^{10}$	2700	0.008	0.00704
Upper bound ( $\alpha = 0$ )				
$f_i$ (Hz)	$7.2 \times 10^{10}$	2700	0.012	0.0096
$\phi_{4808,1}$	$7 \times 10^{10}$	2700	0.008	0.0064
$\phi_{7640,1}$	$7.2 \times 10^{10}$	2800	0.012	0.0064

non-monotonic functional dependencies, large variations and large industrial finite element models, the latter being true when only few specific fuzzy solutions must be studied.

### 7. Conclusion

This paper proposed a new PAEM (Padé Approximants with Extrema Management) method, as an alternative to the Zadeh Extension Principle. This new method allows both fuzzy eigenvalues and fuzzy eigenvectors to be precisely calculated with acceptable CPU times. This method takes two fundamental notions, namely functional dependence and the mode shape pairing, into account and exploits high-order approximations in order to limit the computational costs associated with variability management. Practically, the PAEM method is based on the discretization of parameter membership functions and the search for discrete parameter value combinations, which indicate the minimum and maximum eigensolution variations for each  $\alpha$ -cut level. Efficient Padé approximants are used to calculate these extreme eigensolutions.

Four test cases were evaluated to highlight the efficiency of the proposed method. The first test focused on monotonic and non-monotonic functional dependence, the second on a large variation in the fuzzy parameters, the third one on multiple fuzzy parameters, and the last on a large industrial finite element model. This method has now been applied in a CAD context [35] to optimize the fuzzy solutions in terms of fuzzy restriction rules.

### Appendix

The proposed method uses Padé approximants, which are obtained in the following manner:

- (1) From the vectors  $\mathbf{U}_1, \dots, \mathbf{U}_n$  of Eq. (6), an orthogonal basis is built using the Gram-Schmidt procedure (in the computations,  $n = 3$ ):

$$\begin{cases} \mathbf{U}_1 = \alpha_{11}\mathbf{U}_1^*, \\ \mathbf{U}_2 = \alpha_{21}\mathbf{U}_1^* + \alpha_{22}\mathbf{U}_2^*, \\ \mathbf{U}_3 = \alpha_{31}\mathbf{U}_1^* + \alpha_{32}\mathbf{U}_2^* + \alpha_{33}\mathbf{U}_3^*. \end{cases}$$

Then, this basis is inserted into the polynomial representation, which introduces three polynomials of decreasing degrees (2–0) as factors in the vector field  $\mathbf{U}_k$ :

$$\mathbf{U}_m - \mathbf{U}_0 = \varepsilon\mathbf{U}_1^*(\alpha_{11} + \varepsilon\alpha_{21} + \varepsilon^2\alpha_{31}) + \varepsilon^2\mathbf{U}_2^*(\alpha_{22} + \varepsilon\alpha_{32}) + \varepsilon^3\mathbf{U}_3^*(\alpha_{33}).$$

- (2) The polynomials are replaced by Padé approximants with the same denominator ( $D_2 = d_1 + \varepsilon d_2$ ), as follows:

$$\begin{cases} \alpha_{11} + \varepsilon\alpha_{21} + \varepsilon^2\alpha_{31} \approx \frac{b_0 + \varepsilon b_1}{D_2}, \\ \alpha_{22} + \varepsilon\alpha_{32} \approx \frac{c_0}{D_2}. \end{cases}$$

The coefficients  $b_i$  and  $c_i$  are computed using the same principles as classic Padé approximants; each fraction must have the same Taylor expansions as the corresponding polynomials up to order 2 and 1, respectively:

$$\begin{cases} b_0 = \alpha_{11}, \\ b_1 = \alpha_{21} + \alpha_{11}d_1, \\ c_0 = \alpha_{22}. \end{cases}$$

The coefficients of  $D_2 = d_1 + \varepsilon d_2$  are the solutions of the triangular system:

$$\begin{cases} \alpha_{31} + \alpha_{21}d_1 + \alpha_{11}d_2 = 0, \\ \alpha_{32} + \alpha_{22}d_1 = 0. \end{cases}$$

- (3) After some reorganization, a new form of the previous rational representation that involves only vectors  $\mathbf{U}_k$  and the coefficients  $d_i$  is obtained:

$$\mathbf{U}_m - \mathbf{U}_0 = \varepsilon \frac{D_1}{D_2} \mathbf{U}_1 + \varepsilon^2 \frac{1}{D_2} \mathbf{U}_2.$$

This last equation corresponds to Eq. (10) for a third-order approximation.

## References

- [1] W.L. Oberkampf, K.V. Diegert, K.F. Alvin, B.M. Rutherford, Variability, uncertainty and error in computational simulation, *AIAA/ASME Joint Thermophysics and Heat Transfer Conference, ASME-HTD* 357 (2) (1998) 259–272.
- [2] M. Shinozuka, Monte-Carlo solution of structural dynamics, *Computers & Structures* 2 (1972) 855–874.
- [3] G.I. Shueller, A state-of-the-art report on computational stochastic mechanics, IASSAR Report on Computational Stochastic Mechanics, *Probabilistic Engineering Mechanics* 12 (4) (1997) 197–321.
- [4] B. Sudret, A. Der Kiureghian, Stochastic finite element methods and reliability: a state-of-the-art report, Technical Report UCB/SEMM-2000/08, Department of Civil and Environmental Engineering, University of California, 2000.
- [5] R.E. Moore, *Interval Analysis*, Prentice-Hall, Englewood Cliffs, New York, 1966.
- [6] O. Dessombz, F. Von Herpe, Application de l'arithmétique des intervalles au calcul des réponses dynamiques de systèmes mécaniques incertains, Table Ronde MV2, Approches robustes en dynamique des structures, Paris, 2000.
- [7] Y. Ben-Haim, Design certification with information-gap uncertainties, *Structural Safety* 21 (1999) 269–289.
- [8] L.A. Zadeh, Fuzzy sets, *Information and Control* 8 (1965) 338–353.
- [9] L.A. Zadeh, The concept of a linguistic variable and its application to approximate reasoning—part I, *Information Sciences* 8 (1975) 199–249.
- [10] L.A. Zadeh, The concept of a linguistic variable and its application to approximate reasoning—part II, *Information Sciences* 8 (1975) 301–357.
- [11] L.A. Zadeh, The concept of a linguistic variable and its application to approximate reasoning—part III, *Information Sciences* 9 (1975) 43–80.
- [12] L.A. Zadeh, Fuzzy sets as a basis for a theory of possibility, *Fuzzy Sets and Systems* 1 (1978) 3–28.
- [13] D. Dubois, H. Prade, Fuzzy sets and systems: theory and applications, in: R. Bellman (Ed.), *Mathematics in Science and Engineering*, Academic Press, London, 1980.
- [14] S. Valliappan, T.D. Pham, Fuzzy finite element analysis of a foundation on an elastic soil medium, *International Journal for Numerical and Analytical Methods in Geomechanics* 17 (1993) 771–789.
- [15] T.D. Pham, S. Valliappan, M. Yazdshi, Modeling of fuzzy damping in dynamic finite element analysis, *Proceedings of the IEEE International Conference on Fuzzy Sets*, part 4 (1995) 1971–1978.
- [16] S. Valliappan, T.D. Pham, Elasto-plastic finite element analysis with fuzzy parameters, *International Journal for Numerical and Analytical Methods in Engineering* 38 (1995) 531–548.
- [17] Z. Qiu, I. Elishakoff, Antioptimisation of structures with large uncertain-but-non-random parameters via interval analysis, *Computer Methods in Applied Mechanics and Engineering* 152 (1998) 361–372.
- [18] B. Lallemand, A. Cherki, T. Tison, P. Level, Fuzzy modal finite element analysis of structures with imprecise material properties, *Journal of Sound and Vibration* 220 (2) (1999) 353–364.
- [19] B. Lallemand, G. Plessis, T. Tison, P. Level, Neumann expansion for fuzzy finite element analysis, *Engineering Computations* 16 (5) (1999) 572–583.
- [20] M. Hanss, The Transformation Method for the simulation and analysis of systems with uncertain parameters, *Fuzzy Sets and Systems* 130 (3) (2002) 277–289.
- [21] S. Donders, D. Vandepitte, J. Van de Peer, W. Desmet, Assessment of uncertainty on structural dynamic responses with the short transformation method, *Journal of Sound and Vibration* 288 (2005) 523–549.
- [22] S. Mc William, Anti-optimisation of uncertain structures using interval analysis, *Computers & Structures* 79 (2001) 421–430.
- [23] F. Massa, B. Lallemand, T. Tison, P. Level, Fuzzy eigensolutions of mechanical structures, *Engineering Computations* 21 (1) (2004) 66–77.
- [24] F. Massa, T. Tison, B. Lallemand, A fuzzy procedure for the static design of imprecise structures, *Computer Methods in Applied Mechanics and Engineering* 195 (2006) 925–941.
- [25] H. Padé, Sur la représentation approchée d'une fonction par des fractions rationnelles, *Annales de l'Ecole Normale Sup.* 9 (3) (1892) 3–93.
- [26] G.A. Baker, P.G. Morris, Basic Theory, *Encyclopedia of Mathematics and its Applications*, Addison-Wesley, New York, Vol. 13, 1996.
- [27] A. Najah, B. Cochelin, N. Damil, M. Potier-Ferry, A critical review of asymptotic numerical methods, *Archives of Computational Methods in Engineering* 5 (1) (1998) 31–50.
- [28] I.-W. Lee, G.-H. Jung, An efficient algebraic method for the computation of natural frequency and mode shape sensitivities—part I. Distinct natural frequencies, *Computers & Structures* 62 (3) (1997) 429–435.



- [29] I.-W. Lee, G.-H. Jung, An efficient algebraic method for the computation of natural frequency and mode shape sensitivities—part II. Multiple natural frequencies, *Computers & Structures* 62 (3) (1997) 437–443.
- [30] X. Yang, S. Chen, B. Wu, Eigenvalue reanalysis of structures using perturbations and Padé approximation, *Mechanical Systems and Signal Processing* 15 (2) (2001) 257–263.
- [31] B. Cochelin, N. Damil, M. Potier-Ferry, Asymptotic numerical methods and Padé approximants for non linear elastic structures, *Revue Européenne des Eléments finis* 3 (2) (1994) 281–297.
- [32] R. Jamai, N. Damil, Influence of iterated Gram-Schmidt orthonormalisation in the asymptotic numerical method, *Comptes Rendus Mécanique* 331 (5) (2003) 351–356.
- [33] A. Elhage-Hussein, M. Potier-Ferry, N. Damil, A numerical continuation method based on Padé approximants, *International Journal of Solids and Structures* 37 (2000) 6981–7001.
- [34] <<http://www.matweb.com>, <http://www.efunda.com>>.
- [35] F. Massa, K. Ruffin, B. Lallemand, T. Tison, Fuzzy finite element method: computer aided design application, *Proceedings of ISMA 2006, International Conference on Noise and Vibration Engineering*, Leuven, Belgium, 2006.